Proceedings of the 1999 IEEE
International Conference on Robotics & Automation
Detroit, Michigan • May 1999

Spatial Impedance Control of Redundant Manipulators

Ciro Natale Bruno Siciliano Luigi Villani

PRISMA Lab
Dipartimento di Informatica e Sistemistica
Università degli Studi di Napoli Federico II
Via Claudio 21, 80125 Napoli, Italy
{natale,siciliano,villani}@disna.dis.unina.it
http://disna.dis.unina.it/prisma

Abstract—**This work is focused on impedance control of redundant manipulators. A spatial impedance formulation is presented where general six-degree-of-freedom (dof) end-effector tasks can be handled. A singularity-free angle/axis representation of end-effector orientation is used which allows geometric task consistency to be preserved. An inverse dynamics control with a dynamically consistent inverse of the geometric Jacobian matrix is developed with the adoption of an inner loop acting on the end-effector position and orientation conferring robustness to unmodeled dynamics and external disturbances. Stabilization of null-space velocities is ensured and utilization of redundant degrees of mobility is carried out to optimize an additional task function. Experimental results on a seven-joint industrial robot with force/torque sensor are discussed.**

1. Introduction

Impedance control is a well-established strategy to manage the interaction of the end effector of a robot manipulator with typically unstructured environments. A novel theoretical framework to impose a desired six-dof impedance behaviour for the end-effector translational and rotational motion has been recently proposed [1,2]. The main feature of the resulting spatial impedance is the use of a singularity-free angle/axis representation of end-effector orientation which leads to a physically meaningful definition of the rotational part of the impedance equation and ensures geometric consistency with the given task [3].

In this paper, the spatial impedance formulation is employed for the problem of controlling redundant manipulators. Following the seminal work in [4], the dynamically consistent pseudoinverse of the manipulator Jacobian is considered which has the advantage of producing no null-space accelerations when an external force and moment is applied at the end effector. Thanks to the use of an angle/axis representation of orientation, the geometric Jacobian is considered in lieu of the analytical Jacobian as in the classical operational space approach [5].

Previous interaction controllers for redundant manipulators were developed in the literature, using e.g. the augmented Jacobian [6] or the extended Jacobian [7]. More recently, in [8] a weighted joint space decomposition has been exploited to find a minimal parameterization of null-space joint velocities leading to a dynamic description of the redundant manipulator in a suitably extended task space.

A critical issue when solving redundancy at the acceleration level [9] is the possible generation of internal motions which may eventually cause an unstable behavior [10]. The problem of stabilizing null-space velocities in force control has been tackled in [11] where a null space velocity controller based on a dynamically consistent pseudoinverse of the manipulator Jacobian is designed. This approach is pursued here to developing a spatial impedance control for redundant manipulators.

The impedance controller is designed according to the inverse dynamics strategy, leading to a resolved-acceleration scheme. A modification of the basic scheme by the inclusion of an inner loop acting on the end-effector position and orientation error is devised to confer good robustness to unmodeled dynamics and external disturbances [12].

Experimental tests on a setup comprising a seven-joint industrial robot with open control architecture and a six-axis force/torque wrist sensor have been conducted, and the results in a case study are discussed.

2. Spatial impedance

When the end effector of a robot manipulator interacts with the environment, it is worth considering a desired frame and a compliant frame; then, a mechanical impedance can be introduced which is aimed at imposing a dynamic behavior for the position and orientation displacements between the above two frames.

The mutual position between the compliant frame and the desired frame can be described by the (3×1) position displacement vector

$$\Delta \boldsymbol{p}_{cd} = \boldsymbol{p}_c - \boldsymbol{p}_d, \tag{1}$$

0-7803-5180-0-5/99 $10.00 © 1999 IEEE

which has been referred to the base frame.

The impedance equation is typically chosen so as to impose a dynamic behavior for the position displacement under a (3×1) force vector $\boldsymbol{f}$ at the end effector, i.e.

$$\boldsymbol{M}_p \Delta\ddot{\boldsymbol{p}}_{cd} + \boldsymbol{D}_p \Delta\dot{\boldsymbol{p}}_{cd} + \boldsymbol{K}_p \Delta\boldsymbol{p}_{cd} = \boldsymbol{f}, \qquad (2)$$

where $\boldsymbol{M}_p$, $\boldsymbol{D}_p$ and $\boldsymbol{K}_p$ are (3×3) positive definite matrices representing the equivalent mass, damping, and stiffness, respectively.

In the classical operational space approach, the rotational part of the impedance equation is defined by extending the formal expression of the equation written for the translational part (1) and using a minimal representation of end-effector orientation in terms of three Euler angles. However, as shown in [1], the rotational stiffness may become not well defined even for small orientation displacements and cannot be specified in a consistent way with the task geometry.

A solution to this problem has been proposed in [3], where a class of geometrically meaningful representations of the mutual orientation between the compliant frame and the desired frame is considered. In detail, the rotation matrix describing the orientation of the compliant frame with respect to the desired frame can be expressed in terms the (3×3) rotation matrix

$$\boldsymbol{R}_c^d = \boldsymbol{r}_{cd}^d \boldsymbol{r}_{cd}^{dT} + \left(\boldsymbol{I} - \boldsymbol{r}_{cd}^d \boldsymbol{r}_{cd}^{dT}\right) \cos\theta + \boldsymbol{S}(\boldsymbol{r}_{cd}^d) \sin\theta, \quad (3)$$

where an equivalent rotation by an angle θ about an axis with (3×1) unit vector $\boldsymbol{r}_{cd}^d$ has been considered, $\boldsymbol{I}$ is the (3×3) identity matrix, and $\boldsymbol{S}(\cdot)$ is the (3×3) skew-symmetric matrix operator performing the cross product between two (3×1) vectors. Hence, the orientation displacement can be expressed as the (3×1) vector

$$\boldsymbol{\varepsilon}_{cd}^d = f(\theta) \boldsymbol{r}_{cd}^d, \qquad (4)$$

where $f(\cdot)$ is a strictly increasing smooth scalar function defined in the open interval $]-\theta_M, \theta_M[$ with $\theta_M > 0$ and $f(0) = 0$. A convenient singularity-free choice is $f(\theta) = \sin(\theta/2)$ leading to the unit quaternion $\{\eta_{cd}, \boldsymbol{\varepsilon}_{cd}^d\}$ defined by

$$\eta_{cd} = \cos\frac{\theta}{2} \qquad (5)$$

$$\boldsymbol{\varepsilon}_{cd}^d = \sin\frac{\theta}{2} \boldsymbol{r}_{cd}^d. \qquad (6)$$

Note that $\{\eta_{cd}, \boldsymbol{\varepsilon}_{cd}^d\}$ and $\{-\eta_{cd}, -\boldsymbol{\varepsilon}_{cd}^d\}$ represent the same orientation; hence, the compliant frame is aligned with the desired frame as long as $\eta_{cd} = \pm 1$ and $\boldsymbol{\varepsilon}_{cd}^d = \boldsymbol{0}$.

The impedance equation for the orientation displacement under a (3×1) moment vector $\boldsymbol{\mu}$ at the end effector is given by

$$\boldsymbol{M}_o \Delta\dot{\boldsymbol{\omega}}_{cd}^d + \boldsymbol{D}_o \Delta\boldsymbol{\omega}_{cd}^d + \boldsymbol{K}_o' \boldsymbol{\varepsilon}_{cd}^d = \boldsymbol{\mu}^d, \qquad (7)$$

where $\Delta\boldsymbol{\omega}_{cd}^d$ is the (3×1) angular velocity vector of the compliant frame relative to the desired frame, $\boldsymbol{M}_o$ and $\boldsymbol{D}_o$ are (3×3) positive definite matrices representing the equivalent inertia and damping, and $\boldsymbol{K}_o'$ is an equivalent stiffness which is related to the (3×3) constant positive definite matrix $\boldsymbol{K}_o$ as

$$\boldsymbol{K}_o' = 2\left(\eta_{cd}\boldsymbol{I} + \boldsymbol{S}(\boldsymbol{\varepsilon}_{cd}^d)\right) \boldsymbol{K}_o. \qquad (8)$$

It is worth remarking that $\boldsymbol{K}_o'$ depends on the relative orientation between the compliant frame and the desired frame [2] so as to refer to a constant rotational stiffness $\boldsymbol{K}_o$ defined in a consistent way with the task geometry [13], i.e. $\boldsymbol{K}_o$ can be specified in terms of three scalars representing the stiffness coefficients about three orthogonal axes.

Notice that, differently from (2), the rotational part of the impedance equation (7) has been derived in terms of quantities all referred to the desired frame; this allows the impedance behavior to be effectively expressed in terms of the relative orientation of the compliant frame with respect to the desired frame, no matter what the absolute orientation of the desired frame with respect to the base frame is.

3. Control of redundant manipulators

For an n-dof rigid robot manipulator, the dynamic model can be written in the Lagrangian form

$$\boldsymbol{B}(\boldsymbol{q})\ddot{\boldsymbol{q}} + \boldsymbol{C}(\boldsymbol{q}, \dot{\boldsymbol{q}})\dot{\boldsymbol{q}} + \boldsymbol{d}(\boldsymbol{q}, \dot{\boldsymbol{q}}) + \boldsymbol{g}(\boldsymbol{q}) = \boldsymbol{\tau} - \boldsymbol{J}^T(\boldsymbol{q})\boldsymbol{h}, \quad (9)$$

where $\boldsymbol{q}$ is the $(n \times 1)$ vector of joint variables, $\boldsymbol{B}$ is the $(n \times n)$ symmetric positive definite inertia matrix, $\boldsymbol{C}\dot{\boldsymbol{q}}$ is the $(n \times 1)$ vector of Coriolis and centrifugal torques, $\boldsymbol{d}$ is the $(n \times 1)$ vector of friction torques, $\boldsymbol{g}$ is the $(n \times 1)$ vector of gravitational torques, $\boldsymbol{\tau}$ is the $(n \times 1)$ vector of driving torques, $\boldsymbol{h} = [\,\boldsymbol{f}^T \quad \boldsymbol{\mu}^T\,]^T$ is the $(n \times 1)$ vector of contact forces exerted by the end effector on the environment, and $\boldsymbol{J}$ is the $(6 \times n)$ Jacobian matrix relating joint velocities $\dot{\boldsymbol{q}}$ to the (6×1) vector of end-effector velocities $\boldsymbol{v}_e = [\,\dot{\boldsymbol{p}}_e^T \quad \boldsymbol{\omega}_e^T\,]^T$, i.e.

$$\boldsymbol{v}_e = \boldsymbol{J}(\boldsymbol{q})\dot{\boldsymbol{q}}, \qquad (10)$$

which is assumed to be nonsingular.

Taking the time derivative of (10) gives the kinematics of the manipulator at the acceleration level, i.e.

$$\dot{\boldsymbol{v}}_e = \boldsymbol{J}(\boldsymbol{q})\ddot{\boldsymbol{q}} + \dot{\boldsymbol{J}}(\boldsymbol{q})\dot{\boldsymbol{q}}. \qquad (11)$$

According to the well-known concept of inverse dynamics, the driving torques can be chosen as

$$\boldsymbol{\tau} = \boldsymbol{B}(\boldsymbol{q})\left(\boldsymbol{J}^{\#}(\boldsymbol{q})(\boldsymbol{a}_e - \dot{\boldsymbol{J}}(\boldsymbol{q})\dot{\boldsymbol{q}}) + \boldsymbol{\phi}_n\right) + \boldsymbol{C}(\boldsymbol{q}, \dot{\boldsymbol{q}})\dot{\boldsymbol{q}} + \boldsymbol{d}(\boldsymbol{q}, \dot{\boldsymbol{q}}) + \boldsymbol{g}(\boldsymbol{q}) + \boldsymbol{J}^T(\boldsymbol{q})\boldsymbol{h}. \quad (12)$$

In (12), ϕ_n is a joint acceleration vector lying in the null space of $\boldsymbol{J}$ which can be designed to control the $n-6$ redundant degrees of mobility, whereas $\boldsymbol{a}_e$ is an end-effector acceleration vector which can be designed to control the 6 dof's in the task space, Also, $\boldsymbol{J}^{\#}$ denotes a pseudoinverse of the Jacobian matrix, and contact force and moment measurements are used to compensate for the term $\boldsymbol{h}$ in (9). To this purpose, notice that it is reasonable to assume accurate compensation of the dynamic terms in the model (9), e.g. as obtained by a parameter identification technique.

It is worth remarking that the control law (12) solves redundancy at acceleration level as in [10]. As shown in [14], this approach is equivalent to solving redundancy at torque level as long as the dynamically consistent pseudoinverse of the Jacobian [4] is considered; namely,

$$\boldsymbol{J}^{\#}(\boldsymbol{q}) = \boldsymbol{B}^{-1}(\boldsymbol{q})\boldsymbol{J}^{T}(\boldsymbol{q})\left(\boldsymbol{J}(\boldsymbol{q})\boldsymbol{B}^{-1}(\boldsymbol{q})\boldsymbol{J}^{T}(\boldsymbol{q})\right)^{-1}. \tag{13}$$

This solution has the advantage of producing no null-space accelerations when an external force and moment is applied at the end effector, and such property is particularly relevant in the context of interaction control at issue in the present work.

Folding the control law (12) in (9), in view of the positive definiteness of $\boldsymbol{B}$, gives

$$\ddot{\boldsymbol{q}} = \boldsymbol{J}^{\#}(\boldsymbol{q})\left(\boldsymbol{a}_e - \dot{\boldsymbol{J}}(\boldsymbol{q})\dot{\boldsymbol{q}}\right) + \phi_n. \tag{14}$$

Then, premultiplying both sides of (14) by $\boldsymbol{J}$, accounting for (11), and observing that $\boldsymbol{J}\boldsymbol{J}^{\#} = \boldsymbol{I}$, $\boldsymbol{J}\phi_n = \boldsymbol{0}$ yields

$$\dot{\boldsymbol{v}}_e = \boldsymbol{a}_e, \tag{15}$$

that is a resolved end-effector acceleration.

The new control input can be chosen as $\boldsymbol{a}_e = [\,\boldsymbol{a}_t^T \quad \boldsymbol{a}_r^T\,]^T$ where $\boldsymbol{a}_t$ and $\boldsymbol{a}_r$ are designed to match the assigned impedance for the translational part and the rotational part, respectively. In view of (2), $\boldsymbol{a}_t$ can be taken as

$$\boldsymbol{a}_t = \ddot{\boldsymbol{p}}_c + k_{Vp}\Delta\dot{\boldsymbol{p}}_{ce} + k_{Pp}\Delta\boldsymbol{p}_{ce} \tag{16}$$

being $\Delta\boldsymbol{p}_{ce} = \boldsymbol{p}_c - \boldsymbol{p}_e$ is the position error between the compliant frame and the end-effector frame, where the latter is computed through the manipulator kinematic model

$$\boldsymbol{p}_e = \boldsymbol{p}_e(\boldsymbol{q}). \tag{17}$$

It is worth remarking that k_{Vp}, k_{Pp} are suitable positive gains of an inner position loop, whose reference $\boldsymbol{p}_c$ and its associated derivatives can be computed by forward integration of the translational impedance equation (2) with input $\boldsymbol{f}$ available from the force sensor. Such gains can be set independently of the impedance parameters so as to provide accurate position tracking of $\boldsymbol{p}_c$ and good rejection of disturbances and unmodeled dynamic effects [12].

As regards orientation control, in view of the quaternion-based rotational impedance in (7), $\boldsymbol{a}_r$ can be taken as [1]

$$\boldsymbol{a}_r = \dot{\boldsymbol{\omega}}_c + k_{Vo}\Delta\boldsymbol{\omega}_{ce} + k_{Po}\boldsymbol{R}_e\varepsilon_{ce}^{e} \tag{18}$$

where k_{Vo}, k_{Po} are suitable positive gains, $\Delta\boldsymbol{\omega}_{ce} = \boldsymbol{\omega}_c - \boldsymbol{\omega}_e$, and ε_{ce}^{e} is the vector part of the quaternion that can be extracted from $\boldsymbol{R}_e^T\boldsymbol{R}_c$; the matrix $\boldsymbol{R}_e$ is needed to refer the orientation tracking error to the base frame and can be computed through the manipulator kinematic model

$$\boldsymbol{R}_e = \boldsymbol{R}_e(\boldsymbol{q}). \tag{19}$$

Note that $\boldsymbol{R}_c$, $\boldsymbol{\omega}_c$, $\dot{\boldsymbol{\omega}}_c$ can be computed by forward integration of the differential equation (7).

The final step consists of designing a redundancy resolution controller in terms of the null-space joint accelerations ϕ_n in (12). To this purpose, ϕ_n shall be chosen so as to ensure stabilization of null-space motion [10] and possibly optimization of an additional task function. Consider the matrix $(\boldsymbol{I} - \boldsymbol{J}^{\#}\boldsymbol{J})$ projecting a vector in the null space of $\boldsymbol{J}$, where $\boldsymbol{I}$ now denotes the $(n \times n)$ identity matrix; then, let

$$\boldsymbol{e}_n = \left(\boldsymbol{I} - \boldsymbol{J}^{\#}(\boldsymbol{q})\boldsymbol{J}(\boldsymbol{q})\right)(\gamma - \dot{\boldsymbol{q}}) \tag{20}$$

denote the null-space velocity error where γ is a joint velocity vector which is available for redundancy resolution. The goal is to make $\boldsymbol{e}_n$ asymptotically converge to zero. Taking the time derivative of (20) and using (14) gives the null-space dynamics, i.e.

$$\begin{aligned}\dot{\boldsymbol{e}}_n = &\left(\boldsymbol{I} - \boldsymbol{J}^{\#}(\boldsymbol{q})\boldsymbol{J}(\boldsymbol{q})\right)(\dot{\gamma} - \phi_n) \\ &- \left(\dot{\boldsymbol{J}}^{\#}(\boldsymbol{q})\boldsymbol{J}(\boldsymbol{q}) + \boldsymbol{J}^{\#}(\boldsymbol{q})\dot{\boldsymbol{J}}(\boldsymbol{q})\right)(\gamma - \dot{\boldsymbol{q}})\end{aligned} \tag{21}$$

where $\dot{\boldsymbol{J}}^{\#}$ is a shortcut notation for the time derivative of $\boldsymbol{J}^{\#}$.

Consider the Lyapunov function candidate

$$V = \frac{1}{2}\boldsymbol{e}_n^T\boldsymbol{B}(\boldsymbol{q})\boldsymbol{e}_n. \tag{22}$$

Computing the time derivative of (22) along the trajectories of system (21) yields

$$\dot{V} = \frac{1}{2}\boldsymbol{e}_n^T\dot{\boldsymbol{B}}\boldsymbol{e}_n + \boldsymbol{e}_n^T\boldsymbol{B}\left(\dot{\gamma} - \phi_n - \dot{\boldsymbol{J}}^{\#}\boldsymbol{J}(\gamma - \dot{\boldsymbol{q}})\right), \tag{23}$$

where the dependence on $\boldsymbol{q}$ has been dropped off, and the following identities have been exploited:

$$\boldsymbol{e}_n^T\boldsymbol{B}\boldsymbol{J}^{\#} = \boldsymbol{0}^T \tag{24}$$

$$\boldsymbol{e}_n^T\boldsymbol{B}(\boldsymbol{I} - \boldsymbol{J}^{\#}\boldsymbol{J}) = \boldsymbol{e}_n^T\boldsymbol{B}. \tag{25}$$

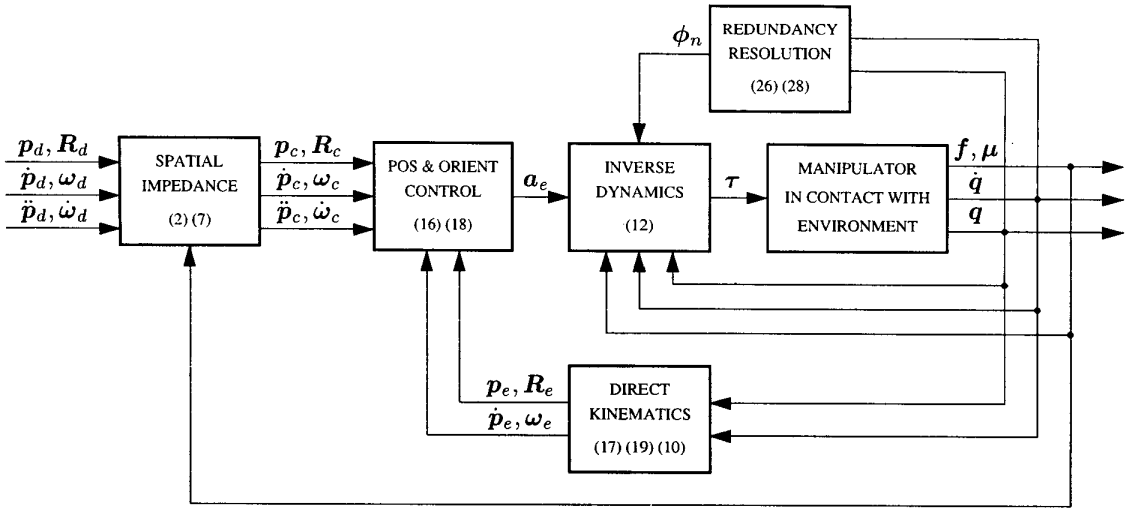

Fig. 1. Spatial impedance control with redundancy resolution.

Choosing

$$\phi_n = (\boldsymbol{I} - \boldsymbol{J}^{\#}\boldsymbol{J})(\dot{\gamma} - \dot{\boldsymbol{J}}^{\#}\boldsymbol{J}(\gamma - \dot{\boldsymbol{q}}) + \boldsymbol{B}^{-1}(\boldsymbol{K}_n\boldsymbol{e}_n + \boldsymbol{C}\boldsymbol{e}_n)) \tag{26}$$

where $\boldsymbol{K}_n$ is a positive definite matrix, and folding it into (23) gives

$$\dot{V} = \frac{1}{2}\boldsymbol{e}_n^T(\dot{\boldsymbol{B}} - 2\boldsymbol{C})\boldsymbol{e}_n - \boldsymbol{e}_n^T\boldsymbol{K}_n\boldsymbol{e}_n = -\boldsymbol{e}_n^T\boldsymbol{K}_n\boldsymbol{e}_n \leq 0 \tag{27}$$

thanks to (25) and the skew-symmetry of the matrix $\dot{\boldsymbol{B}} - 2\boldsymbol{C}$. Therefore, it can be concluded that the choice (26) gives a negative definite $\dot{V}$, and thus $\boldsymbol{e}_n \to \boldsymbol{0}$ asymptotically. It should be said that the proposed control law (26) represents an improvement over the null-space velocity controller proposed in [11] which guaranteed local stability only; a similar result has been independently derived and will be presented in [15].

Regarding the utilization of redundant degrees of mobility, a typical choice for γ is [11]

$$\gamma = k_\gamma \boldsymbol{B}^{-1}\left(\frac{\partial w(\boldsymbol{q})}{\partial \boldsymbol{q}}\right) \tag{28}$$

where k_γ is a signed scalar and $w(\boldsymbol{q})$ is an additional task function that can be locally optimized.

A block diagram summarizing the overall spatial impedance control with redundancy resolution is sketched in Fig. 1.

4. Experiments

The laboratory setup consists of an industrial robot Comau SMART-3 S. having a six-revolute-joint anthropomorphic geometry with nonnull shoulder and elbow offsets and nonspherical wrist.

The manipulator is mounted on a sliding track which provides an additional degree of mobility. The joints are actuated by brushless motors via gear trains; shaft absolute resolvers provide motor position measurements. The robot is controlled by an open version of the industrial controller which is interfaced to a PC Pentium. This is in charge of computing the control algorithm and passing the references to the current servos through the communication link at 1 ms sampling time. Joint velocities are reconstructed through numerical differentiation of joint position readings. A six-axis force/torque sensor ATI FT 130/10 with force range of ± 130 N and torque range of ± 10 Nm is mounted at the wrist of the robot manipulator. The sensor is connected to the PC by a parallel interface board which provides readings of six components of generalized force at 1 ms.

An end effector has been built as a steel stick with a wooden disk of 5.5 cm radius at the tip. The end-effector frame has its origin at the center of the disk and its approach axis normal to the disk surface and pointing outwards.

The proposed spatial impedance control with redundancy resolution has been tested in the following case study. The environment is constituted by a cardboard box. The resulting translational stiffness at the contact between the end effector and the surface is of the order of 5000 N/n, while the rotational stiffness for small angles is of the order of 15 Nm/rad.

The task in the experiment consists of four phases; namely, reconfiguring the manipulator, approaching the surface, staying in contact, and leaving the surface. To begin, the additional task function in (28) has been chosen as

$$w(\boldsymbol{q}) = \frac{1}{2}(q_3 - q_{3d})^2$$

where q_3 is the elbow joint and q_{3d} is a desired trajectory from the initial value of q_3 to the final value of 1.1 rad in a time of 4 s with a 5th-order interpolating polynomial with null initial and final velocity and acceleration. This function is aimed at reconfiguring the manipulator in a more dexterous posture before contacting the surface.

After a lapse of 4 s, the disk is taken in contact with the surface at an angle $\alpha = 7\pi/36$ rad; see Fig. 2 where the orientation of the base and end-effector frames is depicted. The end-effector desired position is required to make a straight line motion with a horizontal displacement of 0.08 m along the z_0 axis of the base frame. The trajectory along the path is generated according to a 5th-order interpolating polynomial with null initial and final velocities and accelerations, and a duration of 2 s. The end-effector desired orientation is required to remain constant during the task. The surface is placed (vertically) in the x_0y_0-plane of the base frame in such a way to obstruct the desired end-effector motion, both for the translational part and the rotational part. After a lapse of 13 s in contact, the end-effector motion is commanded back to the initial position with a duration of 4 s.

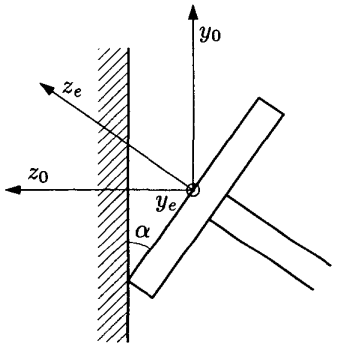

Fig. 2. Disk in contact with surface.

The parameters of the translational part of the spatial impedance equation (2) have been set to $\boldsymbol{M}_p = \text{diag}\{16, 16, 16\}$, $\boldsymbol{D}_p = \text{diag}\{800, 800, 250\}$, $\boldsymbol{K}_p = \text{diag}\{1300, 1300, 800\}$, while the parameters of the rotational part of the spatial impedance equation (7) have been set to $\boldsymbol{M}_o = \text{diag}\{0.7, 0.7, 0.7\}$, $\boldsymbol{D}_o = \text{diag}\{4, 4, 4\}$, $\boldsymbol{K}_o = \text{diag}\{2.5, 2.5, 2.5\}$.

The gains of the inner loop control actions in (16), (18) have been set to $k_{Pp} = 2250$, $k_{Vp} = 70$, $k_{Po} = 4000$, $k_{Vo} = 75$. The gains of the redundancy resolution controller in (26), (28) have been set to $\boldsymbol{K}_n = \text{diag}\{20, 20, 20\}$ and $k_\gamma = 250$.

The results in Fig. 3 show the effectiveness of the proposed spatial impedance control with redundancy resolution. During the reconfiguration (8 s), the components of the position error between the end-effector frame and the desired frame $\Delta\boldsymbol{p}_{ed} = \boldsymbol{p}_e - \boldsymbol{p}_d$ and of the orientation error between the end-effector frame and the desired frame $\boldsymbol{\epsilon}_{ed}^d$ are practically zero, meaning that the dynamics of the null-space motion does not disturb the end-effector motion. Such error remains small during the approach (2 s). During the contact (13 s), the component of the position error along the z_0-axis significantly deviates from zero, as expected; as for the orientation error, the component of the orientation error along the y_e-axis significantly deviates from zero since the end-effector frame has to rotate about y_e in order to comply with the surface. Also, in view of the imposed task, a prevailing component of the contact force can be observed along the z_0-axis after the contact, whereas the sole component of the contact moment about the y_e-axis is significant, as expected. It can be concluded that the compliant behavior is fully consistent with the task geometry [2], and the presence of the inner loop on the end-effector position and orientation provides good rejection of coupling effects caused by disturbances and unmodeled dynamics, e.g. joint friction. During the takeoff (4 s), both the errors and the contact force and moment return to zero.

The same task has been executed again for the spatial impedance control without redundancy resolution ($k_\gamma = 0$). The performance in terms of the contact between the end effector and the surface is substantially the same as above since the additional task does not interfere with the primary interaction task; hence, the time history of the relevant quantities is omitted for brevity. Nevertheless, a comparison between the two cases in Fig. 4 shows that the task function is successfully optimized only when redundancy is exploited.

5. Conclusion

A spatial impedance control with redundancy resolution has been presented in this work. In order to ensure geometric task consistency, the rotational part of the stiffness is described in terms of a unit quaternion. The dynamically consistent pseudoinverse of the manipulator Jacobian is adopted to decouple the dynamics of the end-effector motion from the null-space motion. Redundancy is exploited to stabilize null-space joint velocities and optimize an additional task function. The experimental results for an industrial robot have shown the effectiveness of the approach.

Acknowledgments

Technical discussions with Fabrizio Caccavale are gratefully acknowledged. This work was supported by *Agenzia Spaziale Italiana*.

References

[1] B. Siciliano and L. Villani, "Six-degree-of-freedom impedance robot control," *Proc. 8th Int. Conf. on Advanced Robotics*, Monterey, CA, pp. 387–392, 1997.

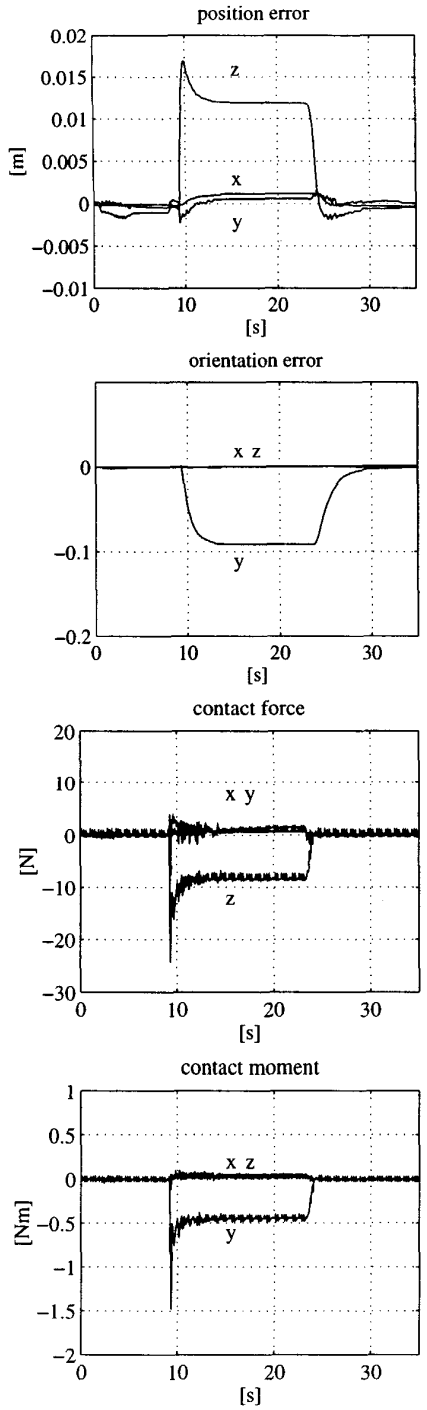

Fig. 3. Experimental results.

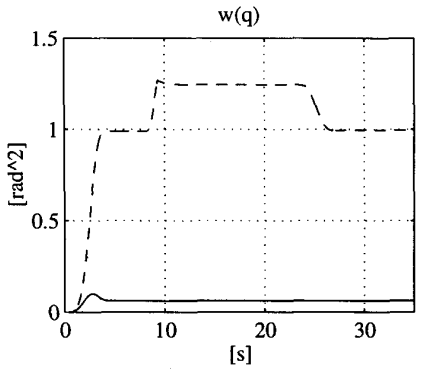

Fig. 4. Additional task function: *solid*—with redundancy; *dashed*—without redundancy.

[2] F. Caccavale, C. Natale, B. Siciliano, and L. Villani "Experiments of spatial impedance control," *Prepr. 5th Int. Symp. on Experimental Robotics*, Barcelona, Spain, pp. 61–72, 1997.

[3] F. Caccavale, C. Natale, B. Siciliano, and L. Villani "Six-dof impedance control based on angle/axis representations," *IEEE Trans. on Robotics and Automation*, submitted for publication, 1998.

[4] O. Khatib, "A unified approach for motion and force control of robot manipulators: The operational space formulation," *IEEE J. of Robotics and Automation*, vol. 3, pp. 43–53, 1987.

[5] L. Sciavicco and B. Siciliano, *Modeling and Control of Robot Manipulators*, McGraw-Hill, New York, NY, 1996.

[6] W.S. Newman and M.E. Dohring, "Augmented impedance control: An approach to compliant control of kinematically redundant manipulators," *Proc. 1991 IEEE Int. Conf. on Robotics and Automation*, Sacramento, CA, pp. 30–35, 1991.

[7] Z.-X. Peng and N. Adachi, "Compliant motion control of kinematically redundant manipulators," *IEEE Trans. on Robotics and Automation*, vol. 9, pp. 831–837, 1993.

[8] Y. Oh, W.K. Chung, Y. Youm, and I.H. Suh, "Motion/force decomposition of redundant manipulator and its application to hybrid impedance control," *Proc. 1998 IEEE Int. Conf. on Robotics and Automation*, Leuven, Belgium, pp. 1441–1446, 1998.

[9] A. De Luca, G. Oriolo, and B. Siciliano, "Robot redundancy resolution at the acceleration level," *Laboratory Robotics and Automation*, vol. 4, pp. 97–106, 1992.

[10] P. Hsu, J. Hauser, and S. Sastry, "Dynamic control of redundant manipulators," *J. of Robotic Systems*, vol. 6, pp. 133–148, 1989.

[11] B. Nemec, "Force control of redundant robots," *Prepr. 5th IFAC Symp. on Robot Control*, Nantes, France, pp. 215–220, 1997.

[12] F. Bruni, F. Caccavale, C. Natale, and L. Villani, "Experiments of impedance control on an industrial robot manipulator with friction," *Proc. 5th IEEE Int. Conf. on Control Applications*, Dearborn, MI, pp. 205–210, 1996.

[13] E.D. Fasse and J.F. Broenink, "A spatial impedance controller for robotic manipulation," *IEEE Trans. on Robotics and Automation*, vol. 13, pp. 546–556, 1997.

[14] R. Featherstone and O. Khatib, "Load independence of the dynamically consistent inverse of the Jacobian matrix," *Int. J. of Robotics Research*, vol. 16, pp. 168–170, 1997.

[15] B. Nemec and L. Žlajpah, "Implementation of force control on redundant robot," *Proc. 1998 IEEE/RSJ Int. Conf. on Intelligent Robots and Systems*, Victoria, B.C., 1998.